




α -Synuclein molecular behavior and nigral proteomic profiling distinguish subtypes of Lewy body disorders

Ivan Martinez-Valbuena¹ · Emily Swinkin² · Enrique Santamaria³ · Joaquin Fernandez-Irigoyen³ · Valerie Sackmann¹ · Ain Kim^{1,4} · Jun Li¹ · Paulina Gonzalez-Latapi^{2,7} · Greg Kuhlman² · Suvorit Subhas Bhowmick² · Naomi P. Visanji^{1,2,4,5} · Anthony E. Lang^{1,2,4} · Gabor G. Kovacs^{1,2,4,5,6} 

Received: 20 April 2022 / Revised: 7 June 2022 / Accepted: 7 June 2022 / Published online: 24 June 2022
© The Author(s), under exclusive licence to Springer-Verlag GmbH Germany, part of Springer Nature 2022

Abstract

Lewy body disorders (LBD), characterized by the deposition of misfolded α -synuclein (α -Syn), are clinically heterogeneous. Although the distribution of α -Syn correlates with the predominant clinical features, the burden of pathology does not fully explain the observed variability in clinical presentation and rate of disease progression. We hypothesized that this heterogeneity might reflect α -Syn molecular diversity, between both patients and different brain regions. Using an ultra-sensitive assay, we evaluated α -Syn seeding in 8 brain regions from 30 LBD patients with different clinical phenotypes and disease durations. Comparing seeding across the clinical phenotypes revealed that hippocampal α -Syn from patients with a cognitive-predominant phenotype had significantly higher seeding capacity than that derived from patients with a motor-predominant phenotype, whose nigral-derived α -Syn in turn had higher seeding capacity than that from cognitive-predominant patients. Interestingly, α -Syn from patients with rapid disease progression (< 3 years to development of advanced disease) had the highest nigral seeding capacity of all the patients included. To validate these findings and explore factors underlying seeding heterogeneity, we performed in vitro toxicity assays, and detailed neuropathological and biochemical examinations. Furthermore, and for the first time, we performed a proteomic-wide profiling of the substantia nigra from 5 high seeder and 5 low seeder patients. The proteomic data suggests a significant disruption in mitochondrial function and lipid metabolism in high seeder cases compared to the low seeders. These observations suggest that distinct molecular populations of α -Syn may contribute to heterogeneity in phenotypes and progression rates in LBD and imply that effective therapeutic strategies might need to be directed at an ensemble of differently misfolded α -Syn species, with the relative contribution of their differing impacts accounting for heterogeneity in the neurodegenerative process.

Keywords Alpha-synuclein · Lewy body disorders · Seeding capacity · Proteomics

✉ Gabor G. Kovacs
gabor.kovacs@uhnresearch.ca

¹ Tanz Centre for Research in Neurodegenerative Disease (CRND), University of Toronto, Krembil Discovery Tower, 60 Leonard Ave, Toronto, ON M5T 0S8, Canada

² Edmond J. Safra Program in PD and the Morton and Gloria Shulman Movement Disorders Clinic, Toronto Western Hospital, Toronto, ON, Canada

³ Clinical Neuroproteomics Unit, Navarrabiomed, Hospital Universitario de Navarra (HUN), Universidad Pública de Navarra (UPNA), Instituto de Investigación Sanitaria de Navarra (IdisNa), Pamplona, Spain

⁴ Department of Laboratory Medicine and Pathobiology, University of Toronto, Toronto, ON, Canada

⁵ Krembil Brain Institute, University Health Network, Toronto, ON, Canada

⁶ Laboratory Medicine Program, University Health Network, Toronto, ON, Canada

⁷ Present Address: Ken and Ruth Davee Department of Neurology, Feinberg School of Medicine, Northwestern University, Chicago, IL, USA

Introduction

Lewy body disorders (LBD) encompass Parkinson's disease (PD), PD with dementia (PDD), and dementia with Lewy bodies (DLB) [2, 25]. Deposition of α -synuclein (α -Syn) into Lewy bodies (LB) and Lewy neurites (LN) is the neuropathological hallmark of these clinically defined conditions [25, 41, 58]. PD is the most common LBD characterized by bradykinesia, rigidity, resting tremor, postural instability, as well as various non-motor symptoms [41]. LBD patients with PD who develop dementia, typically later in the disease course (applying the “one-year rule” after onset of parkinsonism) are considered to have PDD. On the other hand, LBD patients who first develop dementia, with (or without) parkinsonism after 1 year of cognitive or psychiatric symptoms are diagnosed with DLB [24, 34].

α -Syn is a 14 kDa unfolded and soluble cytoplasmic protein enriched in presynaptic nerve terminals that exists as either an intrinsically disordered monomer or an α -helical tetramer [3, 5, 10]. Due to its intrinsically disordered nature, α -Syn can adopt a variety of conformations, including β -sheet-rich structures [17]. Converging evidence implies that in α -Syn-related pathologies, a conformational change (misfolding) of the α -Syn monomer produces an aggregation nucleus (seed) which can recruit endogenous α -Syn molecules and induce their aggregation [46]. These α -Syn seeds can self-propagate and progressively spread between inter-connected brain regions via a variety of mechanisms of cell-to-cell transmission [11, 29] that are believed to generally follow a caudo-rostral pattern [8].

A critical unknown in the basic biology of LBD is an understanding of how the same protein, α -Syn, can be associated with the clinically distinct phenotypes of PD, PDD and DLB. Furthermore, the factors that determine the observed neuroanatomical and cell type vulnerability, such as variability in LB and LN distribution in LBD [8, 34] remain unresolved.

The recent generation of pure fibrillar α -Syn polymorphs with differences in structural and phenotypic traits has led to the hypothesis that different α -Syn strains may be in part responsible for the pathologic and clinical heterogeneity in LBD [7, 14, 28]. The strain hypothesis proposes that the misfolded protein conformation determines which disease a patient will develop [4, 61]. In prion diseases, the kinetics of the prion protein misfolding into each disease-causing conformation typically translates into strain-specific differences in onset and course of the disease [4, 17]. Understanding the structure and molecular nature of these pathological polymorphs in diseased brains will be crucial for the validation of the strain hypothesis

in LBD and for the development of targeted therapeutic interventions. A great leap in resolving the structure of different protein aggregates has recently been provided by advances in cryo-electron microscopy [53, 55, 66]. However, more widely accessible tools to assess the structure and behaviour of the different pathological seeds in different brain regions are still lacking.

One way to identify and study the behavior of potential seeds is to investigate the seeding ability of different misfolded protein species isolated from diseased brains [40]. The underlying hypothesis of this kind of investigation is that aggregates with a higher seeding ability are likely to have a greater role in the spreading of pathology [40].

The property of self-propagation was exploited to establish seeding amplification assays (SAAs) for the detection of disease-associated prion protein (PrP) in human Creutzfeldt–Jakob disease [1]. These SAAs, also known as real-time quaking-induced conversion (RT-QuIC) and protein misfolding cyclic amplification (PMCA), monitor the seeds' propensity to induce aggregation thus amplifying a signal that can sensitively detect minute amounts of these protein seeds using real-time detection of thioflavin T (ThT) fluorescence at multiple timepoints [6, 52].

SAAs have been successfully repurposed to reliably detect other amyloidogenic proteins, such as α -Syn and Tau using a variety of biological samples [27, 31, 33, 46, 49]. Applying these assays to LBD brain homogenates, Sano et al., reported that the α -Syn oligomeric forms, and not the insoluble aggregates, were the active seeding species that triggered the SAA reactions [50]. Candelise et al. observed different SAA kinetics in patients with DLB compared to PD [9]. Moreover, they reported biochemical differences between the α -Syn SAA end-products amplified from DLB and PD patients, suggesting the existence of different α -Syn strains in these diseases [9]. More recently, Sokratian et al. found that, using a novel SAA, an elevated α -Syn fibril activity in cerebrospinal fluid corresponds to reduced survival in DLB [56]. Their results showed a previously unknown heterogeneity of fibril-templating activities in DLB that they postulate may contribute to disease phenotypes [56].

However, to fully investigate this hypothesis, a comprehensive evaluation of the α -Syn seeding capacity across the different brain regions affected in the different clinical subtypes that encompass LBD is required. Thus, in the present study, we systematically evaluated the α -Syn seeding capacity in 8 brain regions from 30 LBD patients with different clinical phenotypes and disease durations. Furthermore, we performed *in vitro* toxicity assays, neuropathological and biochemical examinations and have performed the first substantia nigra (SN) proteotyping from 10 LBD patients with distinct α -Syn seeding capacities.

Materials and methods

Human tissue samples

30 participants (11 females, 19 males) with LBD were selected from the University Health Network–Neurodegenerative Brain Collection (UHN–NBC, Toronto, Canada) based on a definite neuropathological diagnosis. Age at death, sex and details of a complete neuropathologic examination are provided in Supplementary Table 1 (online resource). Autopsy tissue from human brains were collected with informed consent of patients or their relatives and approval of the local institutional review board. This study was approved by the University Health Network Research Ethics Board (Nr. 20–5258). Prior to inclusion in the study, a systematic neuropathological examination was performed following established diagnostic criteria of neurodegenerative conditions and co-pathologies [25]. The contralateral hemisphere was sliced coronally at the time of autopsy and immediately flash frozen and stored at -80°C . Using a 4-mm brain tissue punch, microdissection of the following regions was performed: anterior cingulate cortex, middle frontal cortex, amygdala, hippocampus, middle temporal cortex, SN, pons base, and cerebellar white matter, as previously described [32]. All the punches were stored in low protein binding tubes (Eppendorf, Hamburg, Germany), immediately flash frozen and stored at -80°C .

Clinical data

Clinical charts associated with each case were independently reviewed by movement disorders specialists. Data was extracted including age of onset of motor features, presenting motor phenotype, response to Levodopa, presence of functional surgery, motor complications (dyskinesias, fluctuations, recurrent falls), age of onset of cognitive deficits, affected cognitive domains, presence of hallucinations, age at which dementia documented, age of admission to long-term care, and age of death (Supplementary Table 2, online resource).

Based on these data, cases were subdivided into four clinically distinct groups: (1) motor predominant, corresponding to typical PD ($n=10$, 5 females and 5 males); (2) onset of motor and cognitive symptoms together or within 1 year, corresponding to the “1-year rule” of DLB diagnosis [34] ($n=4$, 1 female and 3 males); (3) cognitive predominant with later emergence of parkinsonism, representative of patients with cognitive impairment who may exhibit parkinsonism as an end-stage result of neurodegeneration or aging, ($n=9$, 3 females and 6 males); (4) cognitive impairment without any motor symptoms ($n=7$, 2 females and 5 males).

Rate of disease progression was determined by the amount of time from the onset of symptoms to a state of advanced disease. Advanced disease was characterized as loss of physical independence due to postural instability/recurrent falls, presence of dementia, or admission to long-term care, whichever came first. Cases with progression to an advanced state of disease within 3 years were characterized as having rapid/malignant progression ($n=6$). As some of the clinical data from older charts was sparse, only cases with robust documentation of the clinical timeline were included in our consideration of disease rate progression.

Protein extraction

For the PBS-soluble fraction, 40–50 mg of frozen micro dissected tissue was thawed on wet ice and then immediately homogenized in 500 μl of PBS spiked with protease (Roche, Basel, Switzerland) and phosphatase inhibitors (Thermo Scientific, Waltham, MA) in a gentle-MACS Octo Dissociator (Miltenyi BioTec, Auburn, CA). The homogenate was transferred to a 1.5-ml low protein binding tube (Eppendorf) and centrifuged at 10,000 g for 10 min at 4°C , as previously described [12, 32]. The supernatant was collected and aliquoted in 0.5-ml low protein binding tubes (Eppendorf) to avoid excessive freeze–thaw cycles. A bicinchoninic acid protein (BCA) assay (Thermo Scientific) was performed to determine the total protein concentration of all samples. For cell culture experiments, PBS-soluble SN extracts containing 100 ng of total α -Syn were pelleted at 150,000g for 30 min at 4°C to sediment seeding species, as previously described [12]. Pellets were subsequently resuspended in 50 μl of PBS and stored at -80°C until further use.

α -Synuclein seeding amplification assay (α -Syn SAA)

SAA reactions were performed in 384-well plates with a clear bottom (Nunc, NY) as previously described [32, 33]. Briefly, full-length human recombinant α -Syn (Impact Biologicals, Swarthmore, PA) was thawed from -80°C storage, reconstituted in HPLC-grade water (Sigma, St. Louis, MI) and filtered through a 100-kDa spin filter (Thermo Scientific) in 500 μl increments. All reagents used in the reaction buffers were purchased from Sigma. 10 μl of the biological sample (5 μg of total protein from the PBS-soluble fraction) was added to the wells containing 20 μl of the reaction buffer (0.1 M PB, pH 8, 0.875 M $\text{Na}_3\text{Citrate}$), 10 μl of 50 μM ThT and 10 μl of 0.5 mg/ml of monomeric recombinant α -Syn. In every plate, positive (1 μg of α -Syn preformed fibrils (rPeptide, Watkinsville, GA)) and negative (deionized water) controls were run. To ensure assay reproducibility, a coefficient of variation no greater than 20% was confirmed when the positive control signals from different runs were compared. The plate was sealed and incubated at

42 °C in a BMG FLUOstar Omega plate reader with cycles of 1 min shaking (400 rpm double orbital) and 1 min rest. ThT fluorescence measurements (450 ± 10 nm excitation and 480 ± 10 nm emission, bottom read) were taken every 15 min for a period of 72 h. Each sample was tested in quadruplicate and the same positive and negative controls were added to each plate.

Histological analysis

4 µm thick formalin-fixed paraffin-embedded tissue sections of neocortical regions, basal ganglia, thalamus, hippocampus, amygdala, midbrain, pons, medulla oblongata, and cerebellum, containing the 8 anatomical regions selected for microdissection (see above) were examined. In addition to Hematoxylin and Eosin-Luxol Fast Blue, a mouse monoclonal antibody for aggregated α -Syn (5G4; 1:4,000 dilution; Roboscreen, Leipzig, Germany) was used for immunohistochemistry. To map the presence of co-pathology with other neurodegenerative disease associated proteins, the following mouse monoclonal antibodies were used: anti-tau AT8 (pS202/pT205; 1:1,000 dilution; Thermo Scientific), anti-phospho-TDP-43 (pS409/410; 1:2,000 dilution; Cosmo Bio, Tokyo, Japan) and anti-A β (clone 6F/3D; 1:50 dilution; Dako, Santa Clara, CA). The EnVision detection kit, Peroxidase/DAB, Rabbit/Mouse (Dako) was used to visualize antibody immunoreactivity. For semi-quantitative analyses of observed pathology and nigral degeneration, we used a 4-point scale: 0, absent; 1, mild; 2, moderate; and 3, severe, as previously described [23, 32]. For the figure, images were taken using Tissuescope™ and were cropped with the HuronViewer™ (Huron, Saint Jacobs, Canada).

ELISA

Human α -Syn Patho and total ELISAs kits (Roboscreen, Leipzig, Germany) were used according to the manufacturer's protocol and as previously described [26].

SDS-PAGE and immunoblotting

Gel electrophoresis was performed using 4–12% Bolt Bis-Tris Plus gels (Thermo Scientific). Proteins were transferred to 0.45-µm nitrocellulose membranes for 60 min at 30 V. Proteins were crosslinked to the membrane via 4% (v/v) paraformaldehyde incubation in PBS for 30 min at room temperature, with rocking. The membranes were blocked for 60 min at room temperature in blocking buffer (5% [w/v] skim milk in 1 × TBST (TBS and 0.05% [v/v] Tween-20)) and then incubated overnight at 4 °C with primary antibodies directed against amino acids 15–123 of the α -Syn protein (1:1,000 dilution, ref: 610,786, BD Biosciences, Franklin Lakes, NJ) [28, 39] or against α -Syn phosphorylated at

Serine 129 (1:1,000 dilution, ref: 015–25,191, Fujifilm Wako, Richmond, VA) diluted in the blocking buffer. The membranes were washed three times with TBST and then incubated for 60 min at room temperature with horseradish peroxidase-conjugated secondary antibodies (1:3000 dilution, ref: 172–1011, Bio-Rad, Hercules, CA) in the blocking buffer. Following another three washes with TBST, immunoblots were developed using Western Lightning enhanced chemiluminescence Pro (PerkinElmer, Waltham, MA) and imaged using X-ray films. For quantification, grayscale images were scanned and imported into Fiji/ImageJ.

Thermolysin and proteinase K digestions

Protease digestions were performed as previously described [28, 39], with minor modifications. A concentration of 25 µg/ml of thermolysin or of 20 µg/ml of proteinase K were added to the PBS-soluble brain homogenates. Samples were incubated at 37 °C with continuous shaking (600 rpm) for 60 min. Thermolysin digestions were halted with the addition of EDTA to a final concentration of 2.5 mM. Proteinase K digestions were halted with a final concentration of 4 mM PMSF. Samples were resuspended in 1 × LDS buffer (Life Technologies, Carlsbad, CA) and analyzed by SDS-PAGE followed by immunoblotting, as described above.

Cell culture and treatment

iCell DopaNeurons (iDopa, Cellular Dynamic International, Madison, WI) were thawed following company guidelines (iCell DopaNeurons User's Guide, Cellular Dynamic International). Cells were plated in complete maintenance medium (Cellular Dynamic International) on a poly-L-ornithine (ref: A004C, Sigma) and laminin (ref: L2020, Sigma) coated 96-well plate (ref: 655090, Greiner Bio-One; Kremsmünster, Austria) at a density of $\sim 4.5 \times 10^5$ cells per well. iDopa cells were maintained and then treated with 2.5% v/v PBS soluble brain homogenates on day in vitro (DIV) 6 and 8. Untreated cells were used as control. On DIV 10, cells were prepared for immunocytochemistry or for cell viability assays.

Toxicity assays

Cytotoxicity was determined by the presence of lactate dehydrogenase (LDH). Supernatant was collected at DIV 8 and 10, spun at 300 g for 5 min and stored at -80 °C. LDH was measured using the Cytotoxicity Detection Kit according to the manufacturer's instructions (ref: 11644793001, Roche, Basel, Switzerland) and absorbance (ABS) was measured at 490 nm and 600 nm using the SpectraMax i3 (Molecular Devices, San Jose, CA). LDH values were calculated using

the equation (ABS 490 nm–ABS 600 nm) sample—(ABS 490 nm–ABS 600 nm) average media blank (background).

Cell viability was determined at DIV 10 using the CellTiter-Blue Cell Viability Assay according to the manufacturer's instructions (ref: 8080, Promega, Madison, WI). In brief, live cells were cultured with 20 μ l of reagent and 100 μ l of medium and incubated for 1 h in standard cell culture conditions. Fluorescence was measured at 560/590 nm (Ex/Em) using the SpectraMax i3 (Molecular Devices). Each biological sample was performed in triplicate for both assays.

Immunofluorescence

Immunofluorescence was performed by first washing the cells in PBS and then fixing with 4% PFA for 10 min at room temperature. Cells were washed 3 times with PBS and incubated in 2% BSA in PBS for 1 h and then in 0.1% TritonX100 + 1% BSA in PBS for 20 min, at room temperature. Samples were incubated with anti-tyrosine hydroxylase (TH, 1:250 dilution, ref: ab137869, Abcam, Cambridge, UK) in 1% BSA in PBS at 4 °C overnight. The following day, cells were washed with PBS and incubated with AlexaFluor-488 donkey–anti-rabbit for 75 min at room temperature (1:500 dilution, ThermoFisher). Finally, cells were washed 4 times in PBS and covered with ProLong Gold Antifade mounting media with DAPI (ref: P36930, Invitrogen). Images were obtained on a widefield microscope (Zeiss AxioObserver, Oberkochen, Germany).

Mass spectrometry

Sample preparation

Using a 4-mm tissue punch, a microdissection of the SN from 10 LBD patients was performed. Samples were homogenized in modified RIPA buffer (2% SDS, 150 mM NaCl, 50 mM Tris pH8). Protein extraction was performed by mechanical disruption using 1.6 mm stainless steel beads in a Bullet Blender (NextAdvance, Troy, NY). Samples were incubated at 60 °C for 30 min and clarified by centrifugation. Tissue extracts were subjected to TCA precipitation as previously described [20]. Washed protein pellets were solubilized in 800 μ l of urea buffer (8 M urea, 150 mM NaCl, 50 mM Tris pH8, 1X Roche complete protease inhibitor). Protein quantitation was performed using Qubit fluorometry (Invitrogen). 50 μ g of lysate from each sample was reduced with 14 mM dithiothreitol at 25 °C for 30 min followed by alkylation with 14 mM iodoacetamide at 25 °C for 45 min in the dark. Then, samples were digested with 2.5 μ g sequencing grade trypsin (Promega) at 37 °C overnight. The digest was cooled to 25 °C and terminated with 5 μ l of formic acid and desalted

using solid phase extraction on a Waters Oasis HLB solid phase extraction plate. Eluted samples were frozen and lyophilized.

Data acquisition

10% of each digest was analyzed by nano LC–MS/MS with a Waters NanoAcquity HPLC system interfaced to a ThermoFisher Fusion Lumos mass spectrometer (ThermoFisher). Peptides were loaded on a trapping column and eluted over a 75 μ m analytical column at 350 nL/min; both columns were packed with Luna C18 resin (Phenomenex, Torrance, CA) and a 120 min gradient was employed. The mass spectrometer was operated in data-dependent mode, with the Orbitrap operating at 60,000 FWHM and 15,000 FWHM for MS and MS/MS, respectively. The instrument was run with a 3 s cycle for MS and MS/MS. Advanced Precursor Determination [16] was employed.

Data processing

Data were processed with MaxQuant version 1.6.14.0 (Max Planck Institute for Biochemistry, Germany) [62]. The MaxQuant output was further processed using the Perseus software (version 1.5.6.0) [63]. Proteins with a cutoff threshold value higher than 1.33 or lower than 0.77 were considered as differentially expressed proteins. All mass spectrometry data files have been deposited to the ProteomeXchange Consortium [64] (<http://proteomecentral.proteomexchange.org>) via the PRIDE partner repository with the dataset identifier PXD034441 and 10.6019/PXD034441. The identification of significantly dysregulated regulatory/metabolic pathways in the SN proteomic data set was made through Metascape platform [68] using default settings (minimum overlap: 3, minimum enrichment: 1.5, $p < 0.01$). The functional protein association network analysis was performed using the STRING tool [59].

Statistics

Statistical analyses were performed using GraphPad Prism (v.9, San Diego, CA) with a significance threshold of $p = 0.05$. SAAs relative fluorescence responses were also analyzed and plotted using the software GraphPad Prism (v.9). Comparisons were made using unpaired two-tailed t tests or one-way ANOVA with Tukey's multiple comparisons test. Two-tailed Spearman r non-parametric correlations were used to correlate different variables obtained from single individuals using SPSS (v.25, Chicago, IL).

Results

Mapping regional α -Syn seeding in LBD

To test our hypothesis that molecular diversity of α -Syn exists in LBD, we studied 30 subjects with a neuropathological diagnosis of LBD (Supplementary Table 1, online resource). Using an ultrasensitive α -Syn SAA, we analyzed 8 different brain regions from each subject to perform a detailed examination of α -Syn seeding across the brains of each patient. We quantified 5 kinetic parameters from each reaction: lag time, growth phase, T50 (which corresponds to the time needed to reach 50% of maximum aggregation), ThT max, and area under the curve (AUC) of the fluorescence response. Each kinetic parameter was calculated as the mean of the values obtained from each quadruplicate. No significant differences were observed in any of these 5 parameters between the positive and negative control samples run on all plates. We defined the AUC as the seeding parameter of interest as it incorporates all the kinetic features of each aggregation reaction, including the speed and extent of aggregation. The AUC values obtained from all 30 subjects included were clustered by brain region and converted into scores of seeding capacity ranging from 0 to 3 representing negative, low, intermediate, or high α -Syn seeding capacity (Supplementary Table 3, online resource). Then, a heatmap of α -Syn seeding was generated to illustrate diversity in the seeding behaviour of α -Syn between the different brain regions (Fig. 1a). We found that the seeding capacity

from the amygdala-derived α -Syn was significantly higher than the α -Syn derived from the rest of the regions examined, with the sole exception of the hippocampal-derived α -Syn ($p = 0.9613$), which displayed the second highest seeding activity (Fig. 1b). The SN was the region with the third highest α -Syn seeding capacity (Fig. 1b). When the different cortices were evaluated, no differences in α -Syn seeding capacity were observed between the middle frontal, middle temporal, and anterior cingulate cortices (Fig. 1b). Finally, the two regions which displayed the lowest seeding capacity were the pons base and the cerebellum (Fig. 1b). No differences in the overall α -Syn seeding capacity were found between male and females ($p = 0.1227$, Supplementary Fig. 1a, online resource).

LBD clinical subtypes present specific patterns of regional α -Syn seeding

Having found evidence of differential α -Syn seeding activity across different brain regions, we next evaluated whether this regional diversity was consistent across different LBD clinical subtypes. The clinical charts associated with each case included in the study were independently reviewed by movement disorders specialists (Supplementary Table 2, online resource). Based on these data, the 30 cases included were subdivided into four clinically distinct groups: (1) motor predominant, corresponding to typical PD ($n = 10$); (2) motor and cognitive onset together or within 1 year, corresponding to the “1-year rule” of DLB diagnosis ($n = 4$); (3) cognitive predominant with later emergence of parkinsonism, representative of patients with cognitive impairment who may

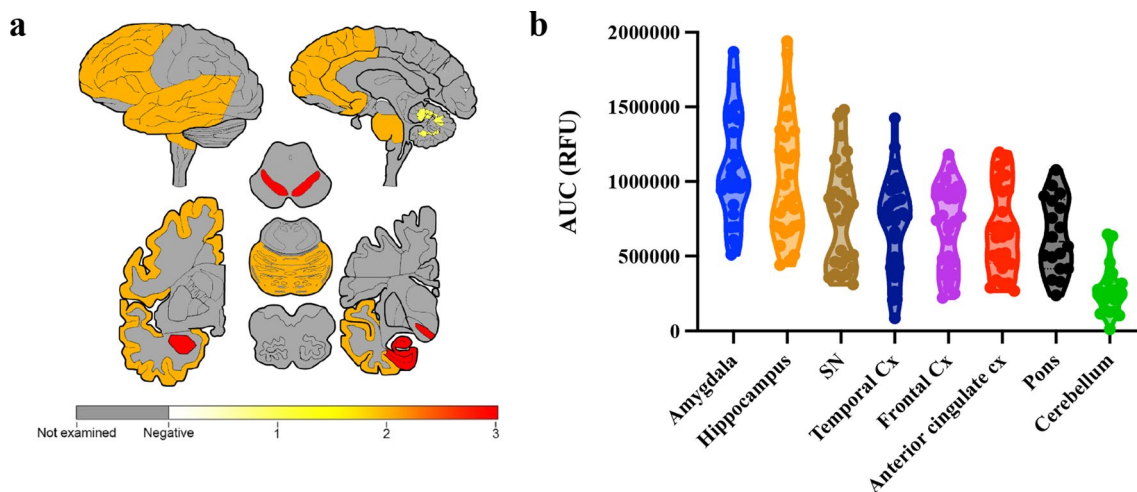


Fig. 1 Extensive heterogeneity of α -Syn seeding activity across different LBD brain regions. Heatmap of α -Syn seeding (a) assessed by SAA. All the area under the curve (AUC) values obtained from the subjects included in the study were clustered by brain region (b) and converted into scores ranging from 0 to 3 to generate the heat-

map. The α -Syn seeding ranged from yellow (low) through orange (medium) to red (high). Grey colored cortical regions indicate that the region was not evaluated. Each dot in b represents an individual biological sample measured in quadruplicate

exhibit parkinsonism as an end-stage result of neurodegeneration or aging ($n=9$); and (4) cognitive only, without any motor symptoms ($n=7$). All AUC values obtained from the α -Syn SAA were clustered by disease subtype (Supplementary Table 3, online resource) and brain region and converted into scores ranging from 0 to 3. Four heatmaps were generated to illustrate the regional diversity of α -Syn seeding across the four different clinical subtypes (Fig. 2a–d). The amygdala had the highest α -Syn seeding capacity in both motor and cognitive predominant subgroups, whereas hippocampal α -Syn had the highest seeding activity in those patients with cognitive impairment without any motor symptoms and those with an onset of motor and cognitive symptoms together or within 1 year (Fig. 2a–d, Supplementary Fig. 2, online resource). The comparison of the seeding capacity across the clinical phenotypes also revealed that hippocampal α -Syn from patients with a cognitive-predominant phenotype had significantly higher seeding capacity than that derived from patients with a motor-predominant phenotype ($p=0.0018$, Fig. 2f), whose nigral-derived α -Syn in turn had higher seeding capacity, although not statistically significant, than that from cognitive-predominant patients (Fig. 2e).

To illustrate the typical profile of α -Syn SAA for LBD subjects with a motor predominant phenotype or with cognitive impairment without any motor symptoms, we plotted SAA data from the hippocampus and the SN from one representative motor and one cognitive case (Fig. 2g). When the α -Syn seeding activity was compared between other regions, no significant differences were found between the three cortices examined across the different clinical subtypes. Furthermore, the pons base and the cerebellum consistently displayed the lowest seeding capacity regardless of the clinical phenotype (Supplementary Fig. 2, online resource).

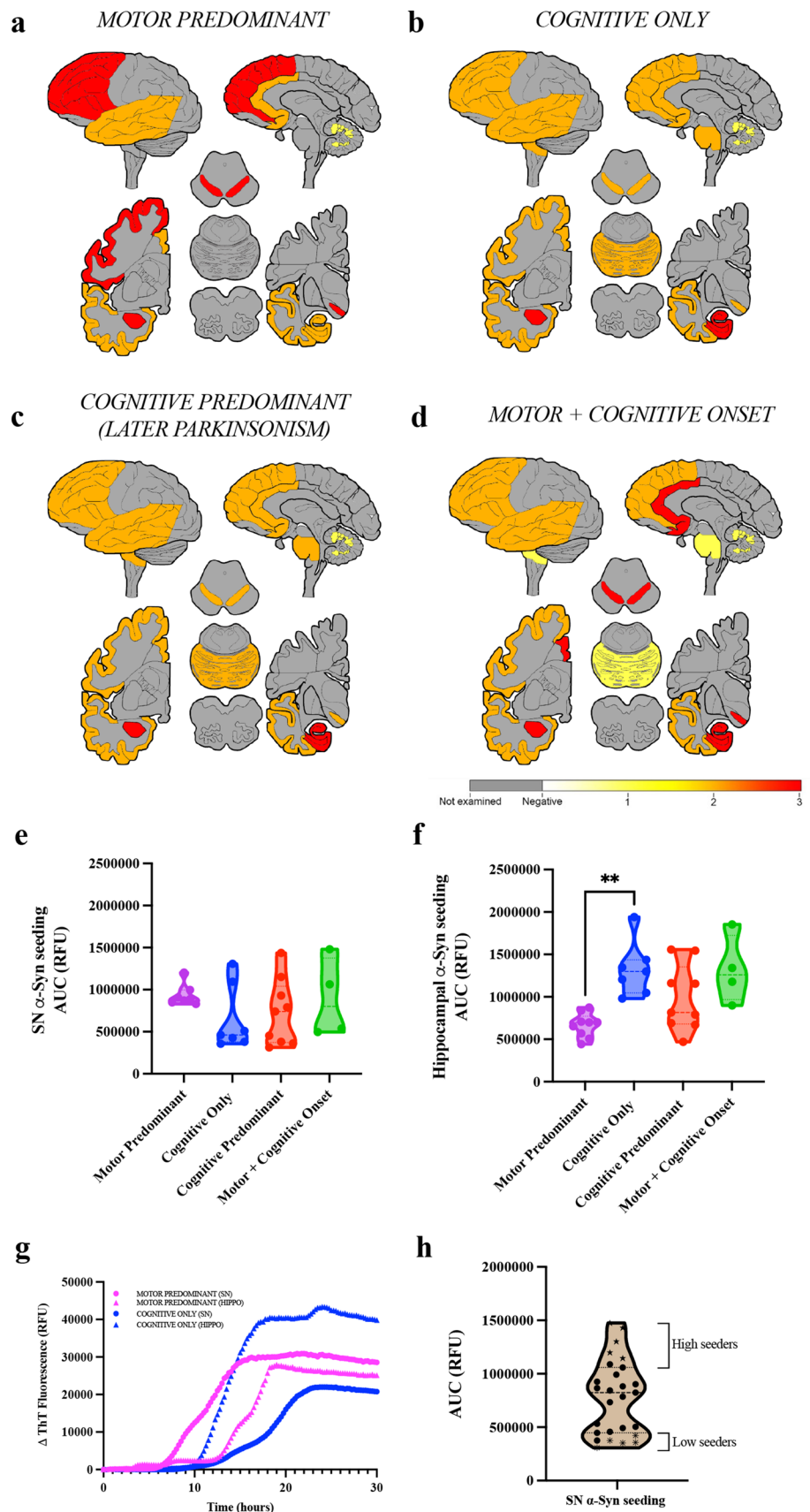
In addition to the observed differences in the AUC among the different brain regions, we also observed up to eight-fold differences in AUC values among the 30 LBD subjects within the same region (Fig. 1b). To test the hypothesis that not only inter-regional but also inter-individual heterogeneity in α -Syn seeding exists in LBD, all 30 LBD cases included in our study were further subtyped into 3 groups: high (those whose AUC values fell within the 3rd quartile), intermediate and low seeders (those whose AUC values fell within the 1st quartile), according to their ability to misfold monomers of recombinant α -Syn in vitro (Fig. 2h). To perform this analysis, we chose to use the SAA data derived from the SN as it is the most consistently affected region in LBD. To assess whether these distinctions could be due to differences in seed concentration or seed characteristics, we performed end-point dilution of the SN PBS-soluble fraction from two LBD cases classified as high and low seeders, respectively (Supplementary Fig. 3, online resource). Regardless of the amount of brain homogenate used to seed the α -Syn SAA

reaction, the seeding activity of the misfolded α -Syn from the high-seeder LBD case was more potent than that from the low-seeder LBD case. Interestingly, when we reviewed the clinical charts from the high and the low seeders, we found that all cases that had a rapid disease progression (<3 years to advanced disease) were categorized as high seeders based on their SN SAA (Supplementary Table 3, online resource). No differences in the nigral α -Syn seeding capacity were found between male and females ($p=0.6796$, Supplementary Fig. 1b, online resource).

Nigral-derived PBS-soluble homogenates from high and low seeders have different cytotoxic properties

To validate our α -Syn SAA results and to evaluate whether the nigral homogenates derived from high and low seeder patients have different cytotoxic profiles, we used human dopaminergic neurons derived from induced pluripotent stem cells (iDOPA cells). We incubated these neurons with brain extracts from 10 LBD patients (5 high and 5 low seeders as defined by the α -Syn SAA). No significant differences in post-mortem delay were found between the two groups of patients ($p=0.9911$, Supplementary Table 1, online resource). We first indirectly titrated the amount of nigral PBS-soluble brain homogenate required to exert some degree of cytotoxicity in these neurons by measuring the concentration of α -Syn. We tested 4 different concentrations of nigral α -Syn (ranging from 0.2 to 2 ng, Supplementary Fig. 4, online resource) derived from a single LBD patient (LBD 14). We observed that the α -Syn concentration needed to produce a significant, but not total, cell loss in this cell line ranged between 0.6 and 1.2 ng. Thus, in further experiments the iDopa cells were exposed to 1 ng of nigral derived α -Syn for 4 days (Fig. 3a). To evaluate the cytotoxic effect of nigral-derived homogenates, we used two different approaches. First, at day in vitro (DIV) 8 and DIV 10 we measured the concentration of lactate dehydrogenase (LDH), as damage of the plasma membrane results in a release of this cytosolic enzyme into the surrounding cell culture medium. When we measured extracellular LDH, we found that at both DIV8 and DIV10 LDH was higher in the cells treated with nigral homogenates derived from either high or low seeder patients compared to control (untreated) cells ($p<0.0001$, Fig. 3b). However, when we compared the LDH levels between LBD patients, we found significantly higher ($p<0.0001$) extracellular LDH expression from the cells exposed to the nigral homogenates derived from the high seeder patients (Fig. 3b). To corroborate these findings, we performed a cell viability assay (CellTiter-Blue[®]) at DIV10. We found a significant decrease in viable iDopa cells exposed to nigral homogenates compared to control (untreated) cells ($p<0.0001$, Fig. 3c). Furthermore, we found a significant decrease in cell viability in iDopa cells

Fig. 2 Regional heterogeneity of α -Syn seeding activity across different LBD clinical subtypes. Area under the curve (AUC) values obtained from the α -Syn SAA were converted into scores ranging from 0 to 3 to generate α -Syn seeding heatmaps. LBD cases were then divided into four clinically distinct groups: **a** motor predominant, **b** cognitive impairment without any motor symptoms, **c** cognitive predominant with later emergence of parkinsonism, and **d** onset of motor and cognitive symptoms together or within 1 year. The AUC values from the substantia nigra (SN) (**e**) and the hippocampus (**f**) from the motor predominant and the cognitive impairment only groups are shown for comparative purposes. **g** Aggregation curves of α -Syn in the presence of nigral and hippocampal homogenates from a representative LBD motor predominant subject and representative LBD patient with cognitive impairment without any motor symptoms. Data are mean of representative subjects measured in quadruplicate. The AUC values from the SN (**h**) from all the subjects included in the study are shown to display the inter-individual α -Syn seeding variability. Each dot in **a–f** and **h** represents an individual biological sample measured in quadruplicate. Stars in **h** depict the 5 LBD subjects selected as high seeders and the asterisks represent the 5 LBD subjects selected as low seeders for further examinations



exposed to nigral homogenates derived from high seeders, compared to those exposed to nigral homogenates derived from low seeders ($p < 0.0001$, Fig. 3c). At DIV 10, neurons were fixed and immunostained using an antibody for the dopaminergic neuronal marker tyrosine hydroxylase (TH, Fig. 3d). We observed qualitatively that the iDopa cells exposed to nigral homogenates derived from low seeders were fewer and more dystrophic compared to untreated dopaminergic neurons (Fig. 3d). Furthermore, iDOPA cells in the wells treated with nigral homogenates derived from high seeder patients were scarce (Fig. 3d). These results extend the findings obtained with the α -Syn SAA and suggest that the α -Syn and other cofactors present in LBD patients possess not only a different seeding capacity but also confer different cytotoxic properties.

Neuropathological and biochemical characterization of nigral α -Syn from high and low seeder LBD patients

As it is yet unknown what causes the α -Syn from a particular patient with LBD to drive higher vs lower seeding, our next step was to perform a detailed neuropathological and biochemical examination of the 10 patients (5 high seeders and 5 low seeders, Supplementary Table 3, online resource) used for the in vitro analysis. First, we evaluated whether the heterogeneity of α -Syn seeding was reflected in the neuropathological findings. To this end, we performed a semi-quantitative evaluation of the α -Syn pathology in the SN from these patients using the 5G4 antibody, which labels disease-associated misfolded forms of α -Syn [26]. Interestingly, there were no significant differences in the burden of α -Syn pathology between the two groups of patients (Fig. 4). Next, we assessed whether any differences in the pattern of nigral co-pathology with other disease associated proteins could be found between the two groups. The presence of concomitant tau and A β pathology was very similar between high and low seeders (Fig. 4). Furthermore, no differences in nigral degeneration were found: 2 low seeders and 1 high seeder presented a mild nigral degeneration, 2 low seeders and 2 high seeders had a moderate nigral degeneration, whereas 1 low seeder and 2 high seeder presented a severe nigral degeneration.

As the histological examination did not yield any differences between high and low seeders, we looked for further biochemical and structural differences in the α -Syn derived from the brain homogenates prepared from high and low seeders. We quantified the amount of total and aggregated α -Syn using ELISA. The 10 LBD cases had 2–3 ng of total α -Syn per mg of tissue in the SN PBS-soluble fraction and no differences in the overall amount of α -Syn were found between high and low seeders (Fig. 5a). The amount of aggregated α -Syn was quantified using the α -Syn Patho

ELISA. LBD cases had 5–200 pg of aggregated α -Syn per mg of tissue in the SN PBS-soluble fraction. Interestingly, the amount of aggregated α -Syn was significantly higher ($p = 0.0079$) in the low seeders compared to the high seeders (Fig. 5b). To validate these results, and to correlate the amount of total and aggregated α -Syn with its seeding behavior in the SN, we quantified both total and aggregated α -Syn in the SN from all the subjects included in the study (Supplementary Fig. 5 a, c, online resource). We grouped the cases by clinical subtypes and no differences in either the levels of total or aggregated α -Syn between the 4 clinical subtypes were found (Supplementary Fig. 5 b, d, online resource). The total amount of α -Syn in the PBS-soluble fraction did not correlate with the α -Syn seeding activity ($p = 0.271$, $r = -0.05$, Supplementary Fig. 6a, online resource). However, the levels of aggregated α -Syn inversely correlated with the α -Syn seeding activity ($p = 0.0169$, $r = -0.4557$, Supplementary Fig. 6b, online resource). We then immunoblotted under denaturing conditions the nigral PBS-soluble protein extracts from the high and low seeders against total α -Syn (Fig. 5c) and phosphorylated Ser129 α -Syn (Fig. 5d). No significant differences in banding patterns were found between the subjects, but the quantification of the phosphorylated Ser129 α -Syn immunoblot revealed a trend in the high seeders to have more phosphorylated α -Syn monomers (~14 kDa) than the low seeders ($p = 0.0549$, Supplementary Fig. 6c, online material). No significant differences in the high molecular weight α -Syn species were found between groups ($p = 0.1888$, Supplementary Fig. 6d, online material). To characterize the physical properties of α -Syn in these SN PBS-soluble homogenates, we employed two protease-sensitivity digestion assays that we have previously used to define different conformations of α -Syn [28, 39]. Nigral homogenates were incubated with different concentrations of proteinase K (20 μ g/ml) or thermolysin (25 μ g/ml). Although the protein extracts from the high and low seeders had similar α -Syn (Fig. 5c) banding patterns when immunoblotted under denaturing conditions, these patterns significantly diverged among groups after treatment with thermolysin (Fig. 5e, $p = 0.0440$, Supplementary Fig. 6e, online material) but not after treatment with proteinase K (Fig. 5f, $p = 0.3326$, Supplementary Fig. 6f, online material). These results indicate inter-individual differences in protease sensitivity between the 10 subjects included and that the α -Syn derived from the high seeder patients trended towards being more resistant to thermolysin digestion.

SN proteotype remodeling between high and low seeders

In our final experiment, we performed mass-spectrometry-based quantitative proteomics to elucidate the molecular mechanisms that might underly the differential α -Syn

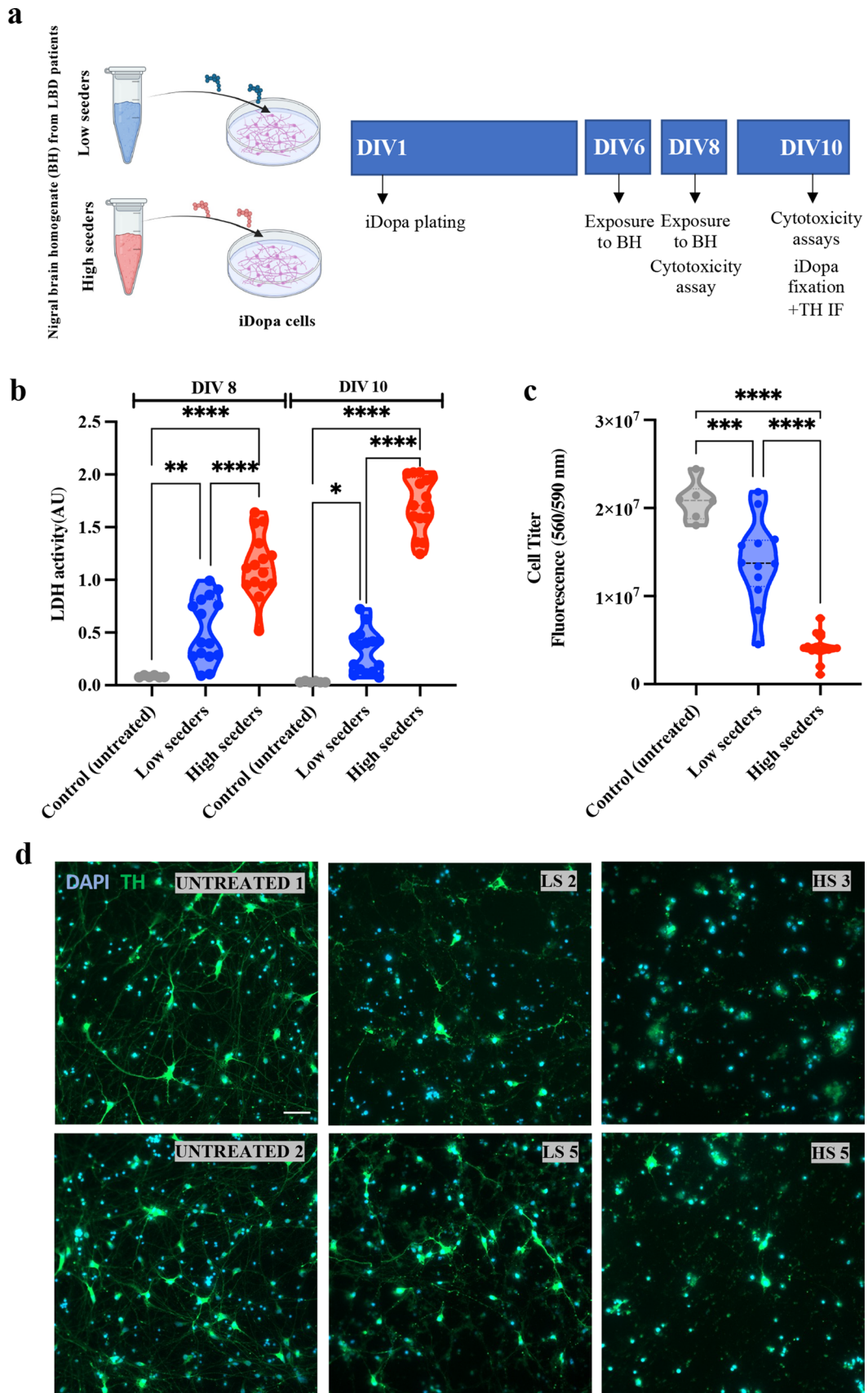


Fig. 3 Nigral brain homogenates derived from high and low seeders impart different levels of cytotoxicity in dopamine neurons. **a** Schematic of experimental design, where human dopaminergic neurons derived from induced pluripotent stem cells (iDOPA cells) were incubated with PBS-soluble nigral derived homogenates extracted from 10 LBD patients (5 high and 5 low seeders as defined in the α -Syn SAA). To evaluate their cytotoxic profiles, **b** at day in vitro (DIV) 8 and DIV 10 the concentration of lactate dehydrogenase (LDH) was measured, as well as, at DIV10 (**c**) a cell viability assay (CellTiter-Blue[®]) was performed to estimate the number of viable cells. **d** Representative confocal photomicrographs of iDopa cells incubated with nigral brain homogenates derived from high and low seeders and immunostained with and antibody for tyrosine hydroxylase (TH) were acquired to complement the cytotoxic assays

seeding capacity observed in LBD. We analyzed the nigral proteome of 10 LBD patients (including 5 high seeders and 5 low seeders) which were previously used for the in vitro experiments, and from which we had a detailed neuropathological and biochemical characterization. Our proteomic analysis identified 2450 proteins in the SN of these patients, of which 78 were differentially expressed in high vs low seeders (Fig. 6a). From these 78 differentially expressed proteins, 36 were more highly expressed in the high seeders compared to low seeders, whereas 42 were more highly expressed in the low seeders compared to the high seeders (Fig. 6b). To elucidate the molecular mechanisms and cellular compartments that differed according to α -Syn seeding capacity, we first performed a subcellular mapping of these differentially expressed proteins. We found that the inner, lumen-facing, lipid bilayer of cellular organelles, as well as the axons, the microtubules and the mitochondrial matrix were significantly enriched subcellular compartments (Fig. 6c, Supplementary Table 4, online resource). Furthermore, we conducted analyses to explore the differential proteome distributions across specific pathways/biofunctions (Fig. 6d). Proteins related to the mitochondrial oxidative phosphorylation (OXPHOS) system, as well as proteins related to mitochondrial apoptosis were differentially expressed between high and low seeders. Furthermore, proteins linked to alterations in microtubule cytoskeleton, as well as in lipid and amino-acid metabolism were found to be significantly dysregulated in the SN of these patients (Fig. 6d, Supplementary Table 5, online resource). Finally, we performed a network analysis to evaluate whether any of the significantly expressed proteins had been previously associated with α -Syn in the literature. Our analysis revealed that from the 78 dysregulated proteins, 10 proteins had been reported to functionally interact with α -Syn (Supplementary Fig. 7, online resource).

Discussion

Our multidisciplinary study has revealed several novel aspects of the behavior of α -Syn in LBD. First, we have provided evidence of a previously unrecognized intra-regional heterogeneity in the seeding activity of α -Syn, with seeding activity varying between different brain regions of a given individual. Second, we describe region specific differences in α -Syn seeding activity between different clinical phenotypes. We confirm that an elevated α -Syn seeding activity correlates with higher cytotoxicity and corresponds to a faster progression of the disease in LBD. Finally, our proteomic analysis has identified a significant disruption in mitochondrial function and lipid metabolism in high seeder LBD patients compared to low seeders patients.

LBD are clinically heterogeneous, and although the distribution of LB and LN might correlate with the predominant clinical features, the burden of α -Syn inclusions does not fully explain the differences in clinical presentation and rate of disease progression exhibited in LBD [13, 35]. Accumulating evidence indicates that the conformational diversity of α -Syn might explain the heterogeneity found in synucleinopathies [18, 65]. As different strains of an increasing number of proteins associated with neurodegenerative diseases have been identified, there is an increasing understanding that conformational diversity appears to be a phenomenon that is common to most neurodegenerative diseases [40]. However, analysing the distribution and interaction of different protein strains in diseased brains is extremely challenging, as we have a limited understanding regarding how different protein assemblies form and what species are most associated with human disease [40]. In recent years, mounting evidence has highlighted an important role of amyloidogenic proteins present in soluble brain fractions in seeding pathologic aggregation, rather than those proteins in the larger-insoluble aggregates [50]. One way to identify and study the behavior of potential seeds is to investigate the seeding ability of different misfolded protein species isolated from diseased brains in vitro [40]. The capacity to monitor in real time how misfolded α -Syn templates the misfolding of monomers has been exploited by several groups to generate SAAs that are able to measure α -Syn seeding kinetics in a wide range of biological samples [9, 19, 31, 46, 47]. However, despite the great sensitivity and reliability of these assays [48], there are some important methodological aspects that need to be considered before a direct comparison between different α -Syn polymorphs or strains is performed using SAAs. Several studies have demonstrated that the selection of the right conditions to conduct the amplification of the seeds is critical to the outcome [32, 35]. Thus, a different microenvironment of the SAA reaction, different

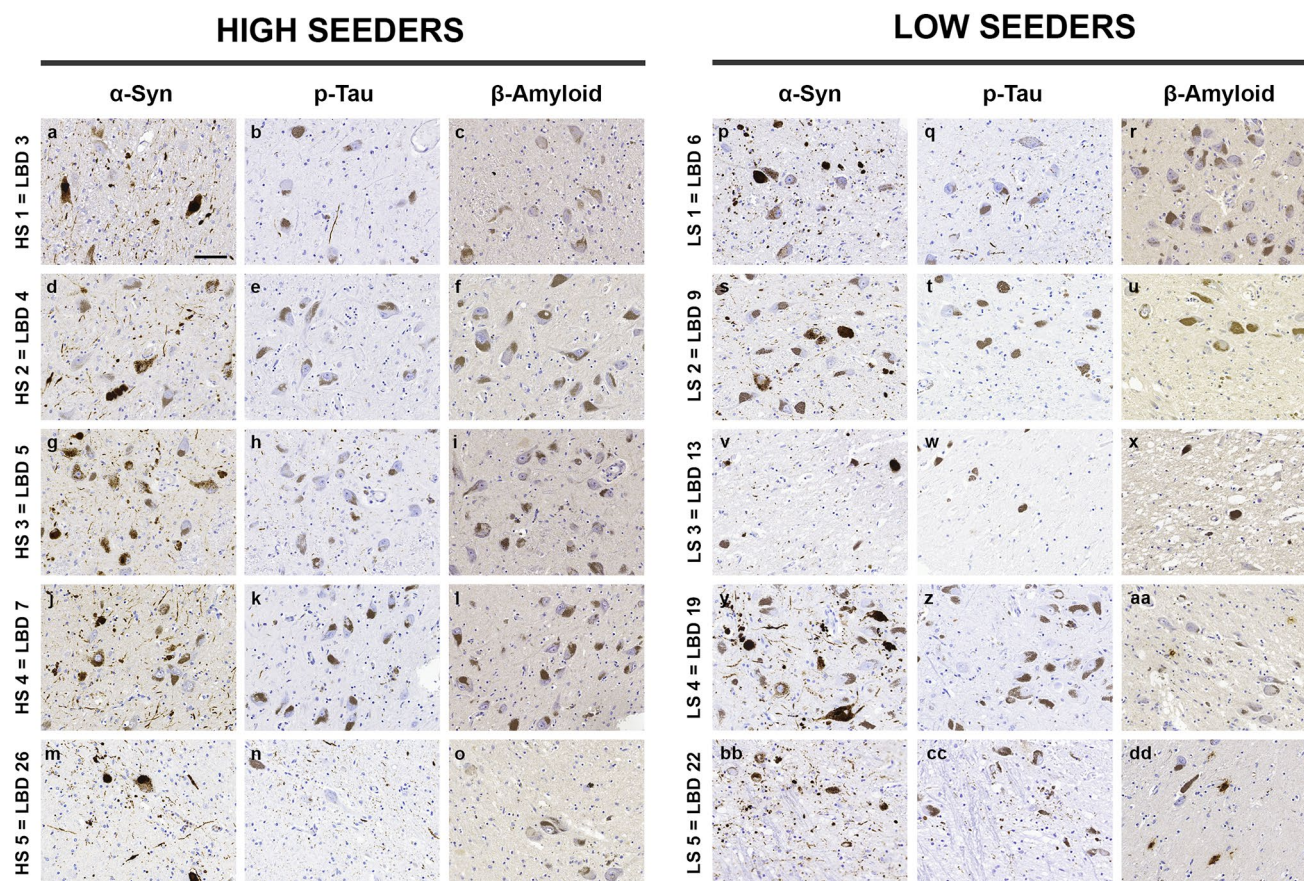


Fig. 4 High and low seeders have similar neuropathological features. Representative immunohistochemistry images for aggregated α -Syn in the substantia nigra (SN) of the 10 LBD patients classified as high seeders (HS 1–5) and low seeders (LS 1–5) as defined by the α -Syn SAA. To evaluate the co-pathology present in these subjects, repre-

sentative immunohistochemistry images of consecutive SN sections stained against phosphorylated tau (p-Tau Ser 202/Thr 205) and amyloid-beta (A-Beta) are shown. Scale bar in 'a' = 50 μ m applies to all images

physical conditions for the aggregation, the use of a different or mutant substrate, or any combination of these factors can yield different results [9]. Indeed, the fact that the physicochemical factors that govern the *in vitro* amplification of α -Syn can be tailored to generate strain-specific reaction buffers can be a great advantage for the development of novel structure-based biomarkers for neurodegenerative diseases [54], but also, the absence of seeding activity could reflect the absence of seeds or might also reflect an inability of the specific SAA conditions to support the amplification of those particular seeds under suboptimal conditions [30]. Thus, in the present study, we conducted the α -Syn SAA using a reaction buffer that has been previously validated for the detection of α -Syn derived from both Multiple System Atrophy (MSA) and LBD patients [33]. Using these validated assay conditions, our study has revealed a hierarchy in the seeding activity of α -Syn in LBD such that α -Syn derived from the amygdala has the highest seeding capacity followed by the hippocampus and the SN. The fact that the α -Syn extracted from one of the most-affected regions in

LBD, the SN, had less seeding capacity than α -Syn derived from both the amygdala and the hippocampus, where less LB and LN are found, could be explained by the circumstance that the α -Syn SAA was performed using the PBS-soluble fraction. It is plausible that the seeding activity of α -Syn could diminish over time as the more soluble seeding-competent α -Syn species, present at earlier stages of disease, become sequestered in larger insoluble aggregates at later stages of the disease [12, 32]. Furthermore, earlier observations using different methodologies have also reported that α -Syn pathology in LBD may be more widespread than can be detected by conventional histopathology [45]. This is supported by our finding of high α -Syn seeding activity in the LBD 29 SN, whose neuropathological examination revealed that the α -Syn pathology was confined only to the amygdala. Surprisingly, no differences in α -Syn cortical seeding capacity were found in LBD patients, however this could be due to the lack of inclusion of other telencephalic structures such as the motor or the occipital cortices.

Having defined regions, where α -Syn seeding capacity was present in LBD, we chose to study the possible contribution of seeding activity to heterogeneity in LBD clinical subtypes. To this end, we subdivided our cohort of 30 LBD patients into four clinically distinct groups: a motor predominant group (corresponding to typical PD); a group whose onset of motor and cognitive symptoms were co-incident or within 1 year, corresponding to the “one-year rule” of DLB diagnosis [34], a group with a cognitive predominant phenotype but with later emergence of parkinsonism, representative of patients with cognitive impairment who may exhibit parkinsonism as an end-stage result of neurodegeneration or aging, and finally a group of patients with cognitive impairment without any motor symptoms. Interestingly, the comparison of seeding activity across the clinical phenotypes revealed that hippocampal α -Syn from patients with a cognitive-predominant phenotype had significantly higher seeding capacity than that derived from patients with a motor-predominant phenotype, whose nigral-derived α -Syn in turn trended towards a higher seeding capacity than that derived from cognitive-predominant patients. Our observed differences in the seeding behavior of α -Syn derived from the nigra and hippocampus between motor and cognitive-predominant patients supports several studies that highlight that brainstem LBs contribute to motor symptoms [38], whereas high densities of parahippocampal LBs are found in demented PD and could even differentiate them from non-demented PD cases with high sensitivity and specificity [15]. However, the relative contributions and interactions of LB and Alzheimer’s disease (AD)-related pathology in this region to memory dysfunction needs to be elucidated [14, 25]. Further studies on the role of α -Syn in the hippocampus of different synucleinopathies will need to be conducted, as our group has also described a high α -Syn seeding capacity in the hippocampus of MSA subjects [32]. Another interesting finding of this study is the high α -Syn seeding capacity found in the amygdala, as this region appears particularly susceptible to neurodegenerative disease pathology [37] and was also previously reported to have a high α -Syn seeding capacity in MSA [32]. Indeed pathologic α -Syn within the amygdala in LBD is unique both in its immunohistochemical properties and immunoblotting profile [57] providing strong support for further studies to fully elucidate the molecular properties of α -Syn in this region.

In addition to the inter-regional α -Syn seeding heterogeneity, our study has also revealed the existence of inter-individual heterogeneity in α -Syn seeding in LBD. We analyzed nigral α -Syn seeding activity in all patients included in the study, and then subclassified these cases into 3 groups: high, intermediate and low seeders, according to their ability to misfold recombinant α -Syn and following the same classification that has previously been applied in MSA [32], DLB [56] and AD [12] patients. Interestingly, when we reviewed

the clinical charts from the cases characterized as high seeders, we found out that all the cases had a rapid disease progression (< 3 years to advanced disease). However, further multicentre studies will be required to validate whether a high α -Syn seeding capacity detected with a SAA correlates with a rapid disease progression or a shorter disease duration.

To further study the characteristics of α -Syn with high seeding activity and α -Syn with low seeding activity, that might contribute to clinical heterogeneity in LBD, we selected 5 LBD patients categorized as high seeders and 5 patients categorized as low seeders. In these 10 LBD patients we performed in vitro cytotoxicity assays followed by a detailed neuropathological and biochemical examination of the SN. To evaluate whether the nigral homogenates derived from high and low seeder patients could exert different cytotoxic properties, we used human dopaminergic neurons derived from induced pluripotent stem cells. After we incubated these neurons with brain extract derived from the SN of these 10 LBD patients, we found a striking decrease in cell viability in the neurons exposed to high seeder-derived nigral homogenates compared to those exposed to nigral homogenates derived from low seeders. However, one limitation of this approach is that the extracts from LBD brains also contained other proteins and lipids, in addition to the pathological α -Syn. Thus, further studies where the α -Syn is immunodepleted from the nigral derived homogenates [42] are required to fully ascertain whether the differential cytotoxic profile found between high and low seeder subjects could have been the result of the action of other co-factors present in the brain extracts.

A detailed neuropathological and biochemical examination was also performed to characterize the α -Syn present in these same 10 LBD patients. First, we aimed to evaluate whether the heterogeneity of α -Syn seeding behavior was reflected in immunohistochemical findings. However, no significant differences were found in the α -Syn burden, or in the presence of concomitant tau or $A\beta$ pathology, between the two groups of patients. This lack of histological differences between the two groups is consistent with previous reports, where no purely immunohistochemical feature distinct of rapidly progressive LBD cases has been found [13]. The lack of histological differences supports the theory that there might be molecular differences between high and low seeders, as a comparable degree of neurodegeneration and amount of protein deposits are detected in all cases, despite a remarkable difference in disease duration. Our study of biochemical and structural differences in the α -Syn brain homogenates found no differences in the overall amount of total α -Syn found between high and low seeders; however, the amount of aggregated α -Syn was significantly higher in the low seeders compared to the high seeders. Furthermore, the levels of aggregated α -Syn were

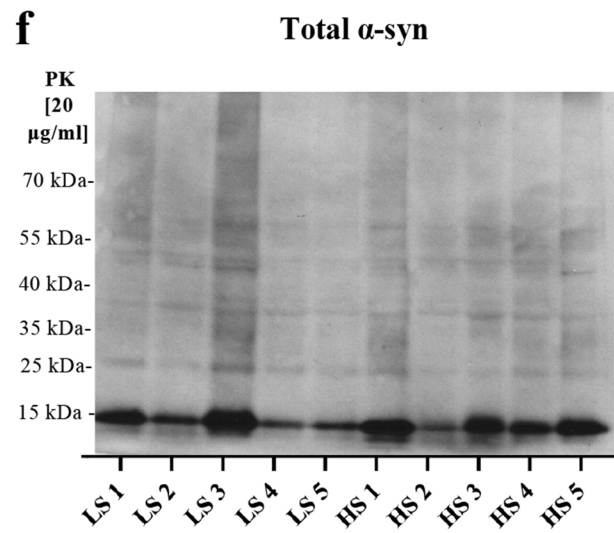
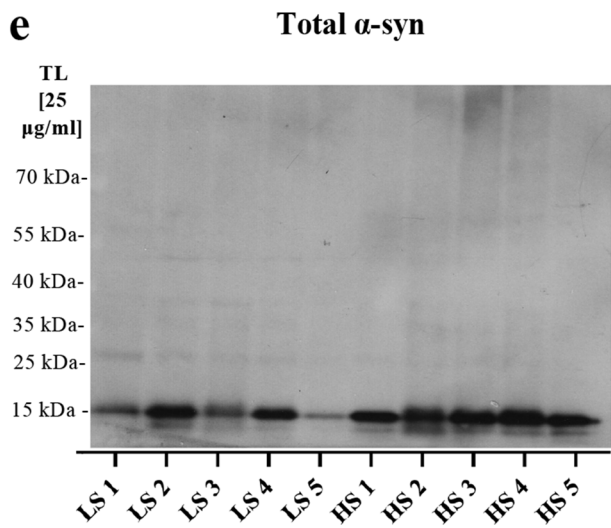
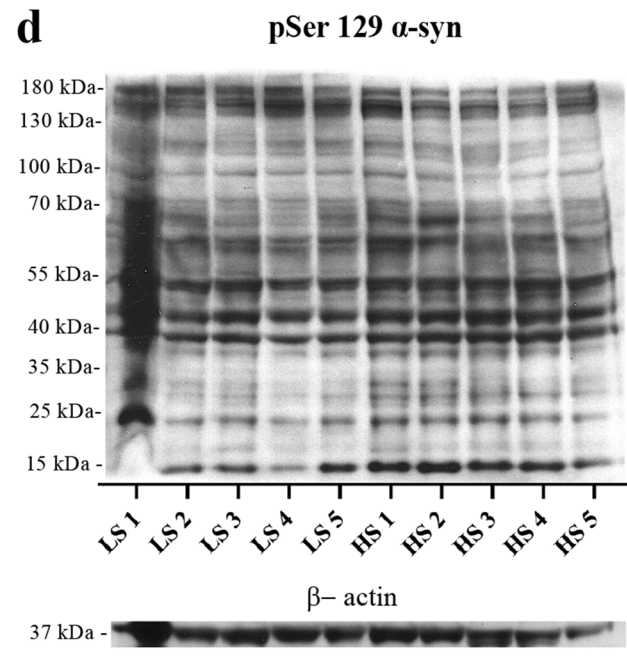
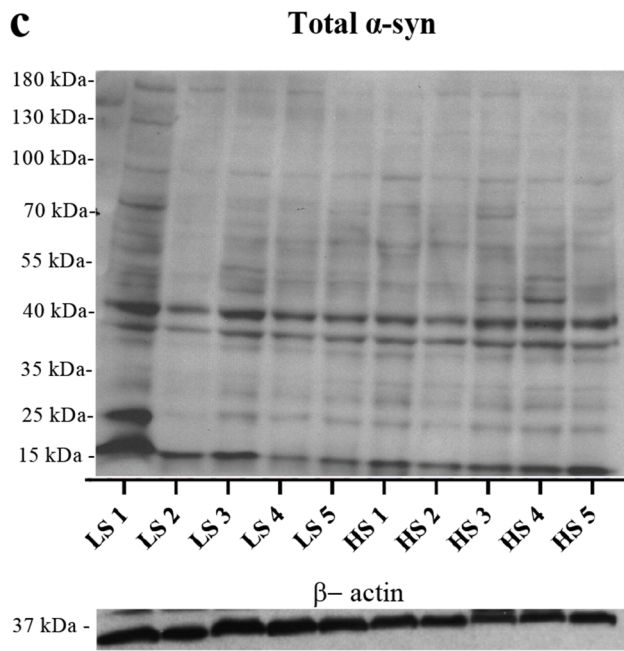
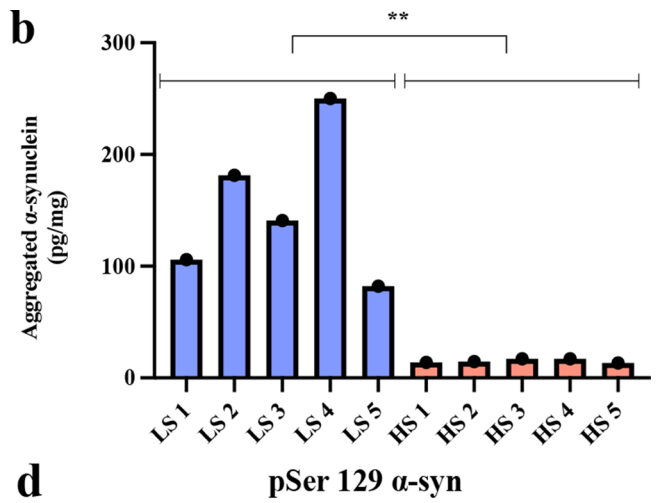
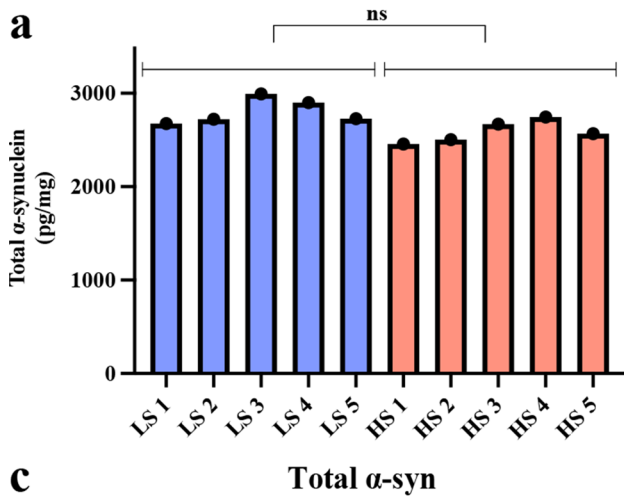


Fig. 5 Biochemical evaluation of α -Syn derived from high and low seeders. **a** Amount of total α -Syn was quantified, using an ELISA assay, in the substantia nigra (SN) of 10 LBD patients classified as high seeders (HS 1–5) and low seeders (LS 1–5) as defined by the α -Syn SAA. **b** Amount of aggregated α -Syn was quantified using the α -Syn Patho ELISA assay in the same region and patients. **c** Representative total α -Syn (Syn-1 clone) and **d** Ser 129 phosphorylated α -Syn (pSer-129 α -Syn), immunoblots showing the banding pattern from the SN PBS-soluble fraction. **e** Representative total α -Syn (Syn-1 clone) immunoblots showing the thermolysin (TL) and **f** proteinase K (PK), digestion of the SN PBS-soluble fraction

negatively correlated with the α -Syn seeding activity in the SN, consistent with our previous findings in MSA patients [32]. To evaluate whether any structural differences in α -Syn could be found between high seeders and low seeders, we used two different protease-sensitivity digestion assays that differentiate protein conformations [28, 39]. We found inter-individual differences in protease sensitivity between the 10 subjects included, and although further studies with a larger number of LBD patients are required, the α -Syn derived from the high seeder patients appeared to be more

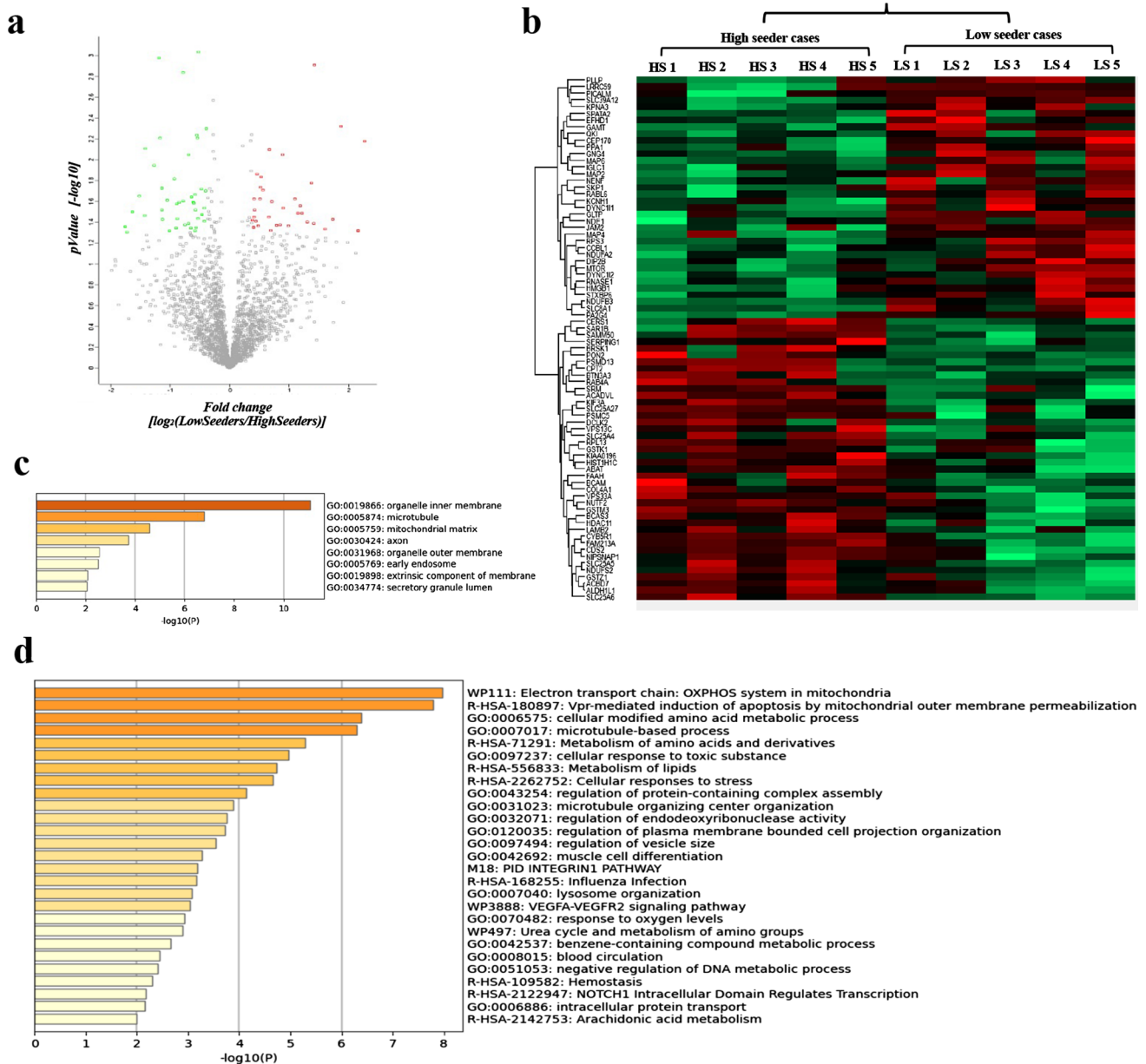


Fig. 6 Substantia nigra proteome remodelling between α -Syn high and low seeders. **a** Volcano plot indicating the statistically significant differentially expressed proteins (DEPs) represented in red (upregulation) and green (downregulation). **b** Heatmap representation showing

both clustering and the degree of change for the DEPs. **c** Subcellular mapping of DEPs. **d** Top 20 pathways and biofunctions significantly enriched in the differential expressed proteome

resistant to thermolysin digestion, analogous with what has been described for tau protein in rapidly progressive AD cases [12, 22].

Our data support the hypothesis that different biologically active conformers of α -Syn exist across LBD brains, raising the intriguing possibility that different underlying pathophysiological mechanisms might occur in different subsets of patients, representing a biological basis for differences in the clinical course. To test this exciting hypothesis, we performed mass-spectrometry-based quantitative proteomics and analyzed the nigral proteome of the 10 LBD patients that were previously used for the *in vitro* experiments, and from which we had a detailed neuropathological and biochemical characterization. Our analysis found that 78 proteins were differentially expressed in high vs low seeders. Interestingly, we found that the inner, lumen-facing, lipid bilayer of cells organelles, as well as the axons, the microtubules and the mitochondrial matrix were the most affected subcellular compartments. Furthermore, an analysis to explore the differential proteome distributions across specific pathways/biofunctions revealed that the majority of differentially expressed proteins were related to the mitochondrial OXPHOS system, a critical mitochondrial system which is responsible for electron transport and generation of the proton gradient in the mitochondrial intermembrane space [60]. Our data also highlight several proteins related to mitochondrial apoptosis and proteins linked to lipid and amino-acid metabolism. The fact that several mitochondrial processes are altered, as well as changes in lipid metabolism and in the lipid bilayer of organelles is consistent with previous reports [51, 67]. Mitochondrial dysfunction is a well-recognized initiating factor of dopaminergic neuronal degeneration and the interplay between mitochondria and α -Syn plays a central role in neuroinflammation [44]. Although the process of LB formation is not yet fully understood, binding of α -Syn to lipid membranes is thought to be a key mediator of oligomerization and aggregation of α -Syn [21, 36]. Interestingly, lipid membranes can promote α -Syn aggregation, and α -Syn oligomer species result in membrane permeabilization, which can disrupt membrane integrity [43]. It is, however, important to note that despite highlighting processes consistent with current concepts of neurodegenerative disease, a major limitation of the current approach is that we are unable to determine whether the observed changes in the proteome are a cause or a consequence of the different α -Syn species found in each patient. Further studies will need to evaluate the role of these differentially expressed proteins found in the high seeders and the low seeders to fully elucidate the mechanism or mechanisms that trigger the development of a rapidly vs slowly progressive disease.

Our multi-disciplinary approach extends our understanding of the contribution of α -Syn diversity to the pathology of LBD, which was previously limited to that demonstrated

using conventional immunohistochemistry. Our work provides strong support for the concept of molecular subtyping of LBD. Using this novel and multi-pronged strategy, we have revealed unexpected differences in seed-competent α -Syn across a cohort of neuropathologically comparable LBD brains. Understanding the relationship between the seeding differences and biological activity of α -Syn will be critical for future subclassification of LBD, which, as proposed by our group for MSA [32], should go beyond the conventional clinical and neuropathological phenotyping and consider the structural and biochemical heterogeneity of α -Syn present in these patients. Such an approach will facilitate the development of new personalized therapeutic strategies that might need to be directed at an ensemble of differently misfolded seeding competent α -Syn species, with the relative contribution of their differing impacts accounting for heterogeneity in the neurodegenerative process. Furthermore, a deeper understanding of how physicochemical factors influence the aggregation of different α -Syn strains will provide support for the development of vitally needed, rapid and structure-based assays for the future diagnosis of LBD and other neurodegenerative diseases.

Supplementary Information The online version contains supplementary material available at <https://doi.org/10.1007/s00401-022-02453-0>.

Acknowledgements The authors particularly acknowledge the patients and their families for their donation. We would also like to acknowledge Dr. Michael Ford and MS Bioworks for their support with the mass spectrometry. Figure 3a was designed with BioRender.com.

Funding This study was supported by the Edmond J. Safra Philanthropic Foundation, the Krembil Foundation, the Rossy Foundation, the Maybank Foundation (to G.G.K. and A.E.L.), the Blidner Family Foundation (to N.P.V.), the Canadian Foundation for Innovation (CFI) John R. Evans Leaders Fund (40480) and the Ontario Research Fund for Small Infrastructure Funds (to G.G.K.). E.S. and J.F.-I. were supported by a grant from the Spanish Ministry of Science Innovation and Universities (Ref. PID2019-110356RB-I00/AEI/10.13039/501100011033). The funding bodies did not take part in design of the study, in collection, analysis, or interpretation of data, or in writing the manuscript.

Declarations

Conflict of interest Gabor G. Kovacs is member of the Acta Neuropathologica Editorial Board but was not involved in the editorial handling of this article. GGK holds a shared patent for the 5G4 synuclein antibody.

References

1. Atarashi R, Wilham JM, Christensen L, Hughson AG, Moore RA, Johnson LM et al (2008) Simplified ultrasensitive prion detection by recombinant PrP conversion with shaking. *Nat Methods* 5:211–212. <https://doi.org/10.1038/nmeth0308-211>
2. Attems J, Toledo JB, Walker L, Gelpi E, Gentleman S, Halliday G et al (2021) Neuropathological consensus criteria for the

- evaluation of Lewy pathology in post-mortem brains: a multi-centre study. *Acta Neuropathol* 141:159–172. <https://doi.org/10.1007/s00401-020-02255-2>
3. Bartels T, Choi JG, Selkoe DJ (2011) α -Synuclein occurs physiologically as a helically folded tetramer that resists aggregation. *Nature* 477:107–110. <https://doi.org/10.1038/nature10324>
 4. Bartz JC (2016) Prion strain diversity. *Cold Spring Harb Perspect Med* 6:a024349. <https://doi.org/10.1101/cshperspect.a024349>
 5. Bendor JT, Logan TP, Edwards RH (2013) Review: The FUNCTION of α -synuclein. *Neuron* 79:1044–1066. <https://doi.org/10.1016/j.neuron.2013.09.004>
 6. Bongianini M, Orrù C, Groveman BR, Sacchetto L, Fiorini M, Tonoli G et al (2017) Diagnosis of human prion disease using real-time quaking-induced conversion testing of olfactory mucosa and cerebrospinal fluid samples. *JAMA Neurol* 74:155–162. <https://doi.org/10.1001/jamaneurol.2016.4614>
 7. Bousset L, Pieri L, Ruiz-Arlandis G, Gath J, Jensen PH, Habenstein B et al (2013) Structural and functional characterization of two α -synuclein strains. *Nat Commun* 4:2575. <https://doi.org/10.1038/ncomms3575>
 8. Braak H, Del Tredici K, Rüb U, De Vos RAI, Jansen Steur ENH, Braak E (2003) Staging of brain pathology related to sporadic Parkinson's disease. *Neurobiol Aging* 24:197–211. [https://doi.org/10.1016/S0197-4580\(02\)00065-9](https://doi.org/10.1016/S0197-4580(02)00065-9)
 9. Candélice N, Schmitz M, Llorens F, Villar-Piqué A, Cramm M, Thom T et al (2019) Seeding variability of different α -synuclein strains in synucleinopathies. *Ann Neurol* 85:691–703. <https://doi.org/10.1002/ana.25446>
 10. Clayton DF, George JM (1999) Synucleins in synaptic plasticity and neurodegenerative disorders. *J Neurosci Res* 58:120–129
 11. Desplats P, Lee H-J, Bae E-J, Patrick C, Rockenstein E, Crews L et al (2009) Inclusion formation and neuronal cell death through neuron-to-neuron transmission of α -synuclein. *Proc Natl Acad Sci* 106:13010–13015. <https://doi.org/10.1073/pnas.0903691106>
 12. Dujardin S, Commins C, Lathuilière A, Beerepoot P, Fernandes AR, Kamath TV et al (2020) Tau molecular diversity contributes to clinical heterogeneity in Alzheimer's disease. *Nat Med* 26:1256–1263. <https://doi.org/10.1038/s41591-020-0938-9>
 13. Gaig C, Valldeoriola F, Gelpi E, Ezquerro M, Lufriu S, Buongiorno M et al (2011) Rapidly progressive diffuse Lewy body disease. *Mov Disord* 26:1316–1323. <https://doi.org/10.1002/mds.23506>
 14. Guo JL, Covell DJ, Daniels JP, Iba M, Stieber A, Zhang B et al (2013) Distinct α -synuclein strains differentially promote tau inclusions in neurons. *Cell* 154:103–117. <https://doi.org/10.1016/j.cell.2013.05.057>
 15. Harding AJ, Halliday GM (2001) Cortical Lewy body pathology in the diagnosis of dementia. *Acta Neuropathol* 102:355–363. <https://doi.org/10.1007/s004010100390>
 16. Hebert AS, Thöing C, Riley NM, Kwiecien NW, Shiskova E, Huguet R et al (2018) Improved precursor characterization for data-dependent mass spectrometry. *Anal Chem* 90:2333–2340. <https://doi.org/10.1021/acs.analchem.7b04808>
 17. Holec SAM, Liu SL, Woerman AL (2022) Consequences of variability in α -synuclein fibril structure on strain biology. *Acta Neuropathol* 143:311–330. <https://doi.org/10.1007/s00401-022-02403-w>
 18. Holec SAM, Woerman AL (2020) Evidence of distinct α -synuclein strains underlying disease heterogeneity. *Acta Neuropathol*. <https://doi.org/10.1007/s00401-020-02163-5>
 19. Ishizawa K, Ksiezak-Reding H, Davies P, Delacourte A, Tiseo P, Yen SH et al (2000) A double-labeling immunohistochemical study of tau exon 10 in Alzheimer's disease, progressive supranuclear palsy and Pick's disease. *Acta Neuropathol* 100:235–244. <https://doi.org/10.1007/s004019900177>
 20. Jessie K, Hashim OH, Rahim ZHA (2008) Protein precipitation method for salivary proteins and rehydration buffer for two-dimensional electrophoresis. *Biotechnology (Faisalabad)* 7:686–693. <https://doi.org/10.3923/biotech.2008.686.693>
 21. Killinger BA, Melki R, Brundin P, Kordower JH (2019) Endogenous α -synuclein monomers, oligomers and resulting pathology: let's talk about the lipids in the room. *NPJ Park Dis* 5:23. <https://doi.org/10.1038/s41531-019-0095-3>
 22. Kim C, Haldiman T, Kang S, Hromadkova L, Han ZZ, Chen W et al (2022) Distinct populations of highly potent TAU seed conformers in rapidly progressing Alzheimer's disease. *Sci Transl Med* 14:1–16. <https://doi.org/10.1126/scitranslmed.abg0253>
 23. Klotz S, Fischer P, Hinterberger M, Ricken G, Hönigschnabl S, Gelpi E et al (2021) Multiple system aging-related tau astrogliopathy with complex proteinopathy in an oligosymptomatic octogenarian. *Neuropathology* 41:72–83. <https://doi.org/10.1111/neup.12708>
 24. Koga S, Sekiya H, Kondru N, Ross OA, Dickson DW (2021) Neuropathology and molecular diagnosis of synucleinopathies. *Mol Neurodegener* 16:83. <https://doi.org/10.1186/s13024-021-00501-z>
 25. Kovacs GG (2019) Molecular pathology of neurodegenerative diseases: principles and practice. *J Clin Pathol* 72:725–735. <https://doi.org/10.1136/jclinpath-2019-205952>
 26. Kovacs GG, Wagner U, Dumont B, Pikkariainen M, Osman AA, Streichenberger N et al (2012) An antibody with high reactivity for disease-associated α -synuclein reveals extensive brain pathology. *Acta Neuropathol* 124:37–50. <https://doi.org/10.1007/s00401-012-0964-x>
 27. Kraus A, Saijo E, Metrick MA, Newell K, Sigurdson CJ, Zanusso G et al (2019) Seeding selectivity and ultrasensitive detection of tau aggregate conformers of Alzheimer disease. *Acta Neuropathol* 137:585–598. <https://doi.org/10.1007/s00401-018-1947-3>
 28. Lau A, So RWL, Lau HHC, Sang JC, Ruiz-Riquelme A, Fleck SC et al (2020) α -Synuclein strains target distinct brain regions and cell types. *Nat Neurosci* 23:21–31. <https://doi.org/10.1038/s41593-019-0541-x>
 29. Luk KC, Kehm V, Carroll J, Zhang B, O'Brien P, Trojanowski JQ et al (2012) Pathological α -synuclein transmission initiates Parkinson-like neurodegeneration in nontransgenic mice. *Science* 338:949–953. <https://doi.org/10.1126/science.1227157>
 30. Manca M, Kraus A (2020) Defining the protein seeds of neurodegeneration using real-time quaking-induced conversion assays. *Biomolecules*. <https://doi.org/10.3390/biom10091233>
 31. Manne S, Kondru N, Jin H, Anantharam V, Huang X, Kanthasamy A et al (2020) α -Synuclein real-time quaking-induced conversion in the submandibular glands of Parkinson's disease patients. *Mov Disord* 35:268–278. <https://doi.org/10.1002/mds.27907>
 32. Martínez-Valbuena I, Visanji NP, Kim A, Lau HHC, So RWL, Alshimeri S et al (2022) Alpha-synuclein seeding shows a wide heterogeneity in multiple system atrophy. *Transl Neurodegener* 11:7. <https://doi.org/10.1186/s40035-022-00283-4>
 33. Martínez-Valbuena I, Visanji NP, Olszewska DA, Sousa M, Bhakta P, Vasilevskaya A et al (2022) Combining skin α -synuclein real-time quaking-induced conversion and circulating neurofilament light chain to distinguish multiple system atrophy and Parkinson's disease. *Mov Disord* 37:648–650. <https://doi.org/10.1002/mds.28912>
 34. McKeith IG, Boeve BF, Dickson DW, Halliday G, Taylor J-P, Weintraub D et al (2017) Diagnosis and management of dementia with Lewy bodies. *Neurology* 89:88–100. <https://doi.org/10.1212/WNL.0000000000004058>
 35. Metrick MA, do Carmo Ferreira N, Saijo E, Hughson AG, Kraus A, Orrù C, Miller MW, Zanusso G, Ghetti B, Vendruscolo M, Caughey B, (2019) Million-fold sensitivity enhancement

- in proteopathic seed amplification assays for biospecimens by Hofmeister ion comparisons. *Proc Natl Acad Sci USA* 116:23029–23039. <https://doi.org/10.1073/pnas.19093221160>
36. Musteikytė G, Jayaram AK, Xu CK, Vendruscolo M, Krainer G, Knowles TPJ (2021) Interactions of α -synuclein oligomers with lipid membranes. *Biochim Biophys Acta Biomembr* 1863:183536. <https://doi.org/10.1016/j.bbamem.2020.183536>
 37. Nelson PT, Abner EL, Patel E, Anderson S, Wilcock DM, Kryscio RJ et al (2018) The amygdala as a locus of pathologic misfolding in neurodegenerative diseases. *J Neuropathol Exp Neurol* 77:2–20. <https://doi.org/10.1093/jnen/nlx099>
 38. Parkkinen L, Kauppinen T, Pirttilä T, Autere JM, Alafuzoff I (2005) α -Synuclein pathology does not predict extrapyramidal symptoms or dementia. *Ann Neurol* 57:82–91. <https://doi.org/10.1002/ana.20321>
 39. Peng C, Gathagan RJ, Covell DJ, Medellin C, Stieber A, Robinson JL et al (2018) Cellular milieu imparts distinct pathological α -synuclein strains in α -synucleinopathies. *Nature* 557:558–563. <https://doi.org/10.1038/s41586-018-0104-4>
 40. Peng C, Trojanowski JQ, Lee VMY (2020) Protein transmission in neurodegenerative disease. *Nat Rev Neurol* 16:199–212. <https://doi.org/10.1038/s41582-020-0333-7>
 41. Poewe W, Seppi K, Tanner CM, Halliday GM, Brundin P, Volkman J et al (2017) Parkinson disease. *Nat Rev Dis Prim* 3:17013. <https://doi.org/10.1038/nrdp.2017.13>
 42. Recasens A, Dehay B, Bové J, Carballo-Carbajal I, Dovero S, Pérez-Villalba A et al (2014) Lewy body extracts from Parkinson disease brains trigger α -synuclein pathology and neurodegeneration in mice and monkeys. *Ann Neurol* 75:351–362. <https://doi.org/10.1002/ana.24066>
 43. Reynolds NP, Soragni A, Rabe M, Verdes D, Liverani E, Hand-schin S et al (2011) Mechanism of membrane interaction and disruption by α -synuclein. *J Am Chem Soc* 133:19366–19375. <https://doi.org/10.1021/ja2029848>
 44. Risiglione P, Zinghirino F, Di Rosa MC, Magri A, Messina A (2021) Alpha-synuclein and mitochondrial dysfunction in Parkinson's disease: the emerging role of VDAC. *Biomolecules* 11:718. <https://doi.org/10.3390/biom11050718>
 45. Roberts RF, Wade-Martins R, Alegre-Abarrategui J (2015) Direct visualization of alpha-synuclein oligomers reveals previously undetected pathology in Parkinson's disease brain. *Brain* 138:1642–1657. <https://doi.org/10.1093/brain/awv040>
 46. Rossi M, Candelise N, Baiardi S, Capellari S, Giannini G, Orrù CD et al (2020) Ultrasensitive RT-QuIC assay with high sensitivity and specificity for Lewy body-associated synucleinopathies. *Acta Neuropathol* 140:49–62. <https://doi.org/10.1007/s00401-020-02160-8>
 47. van Rumund A, Green AJE, Fairfoul G, Esselink RAJ, Bloem BR, Verbeek MM (2019) α -Synuclein real-time quaking-induced conversion in the cerebrospinal fluid of uncertain cases of parkinsonism. *Ann Neurol* 85:777–781. <https://doi.org/10.1002/ana.25447>
 48. Russo MJ, Orru CD, Concha-Marambio L, Giaisi S, Groveman BR, Farris CM et al (2021) High diagnostic performance of independent alpha-synuclein seed amplification assays for detection of early Parkinson's disease. *Acta Neuropathol Commun* 9:1–13. <https://doi.org/10.1186/s40478-021-01282-8>
 49. Saijo E, Ghetti B, Zanusso G, Oblak A, Furman JL, Diamond MI et al (2017) Ultrasensitive and selective detection of 3-repeat tau seeding activity in Pick disease brain and cerebrospinal fluid. *Acta Neuropathol* 133:751–765. <https://doi.org/10.1007/s00401-017-1692-z>
 50. Sano K, Atarashi R, Satoh K, Ishibashi D, Nakagaki T, Iwasaki Y et al (2018) Prion-like seeding of misfolded α -synuclein in the brains of dementia with lewy body patients in RT-QUIC. *Mol Neurobiol* 55:3916–3930. <https://doi.org/10.1007/s12035-017-0624-1>
 51. Schapira AHV (2010) Complex I: Inhibitors, inhibition and neurodegeneration. *Exp Neurol* 224:331–335. <https://doi.org/10.1016/j.expneurol.2010.03.028>
 52. Schmitz M, Cramm M, Llorens F, Müller-Cramm D, Collins S, Atarashi R et al (2016) The real-time quaking-induced conversion assay for detection of human prion disease and study of other protein misfolding diseases. *Nat Protoc* 11:2233–2242. <https://doi.org/10.1038/nprot.2016.120>
 53. Schweighauser M, Shi Y, Tarutani A, Kametani F, Murzin AG, Ghetti B et al (2020) Structures of α -synuclein filaments from multiple system atrophy. *Nature* 585:464–469. <https://doi.org/10.1038/s41586-020-2317-6>
 54. Shahnawaz M, Mukherjee A, Pritzkow S, Mendez N, Rabadia P, Liu X et al (2020) Discriminating α -synuclein strains in Parkinson's disease and multiple system atrophy. *Nature* 578:273–277. <https://doi.org/10.1038/s41586-020-1984-7>
 55. Shi Y, Zhang W, Yang Y, Murzin AG, Falcon B, Kotecha A et al (2021) Structure-based classification of tauopathies. *Nature* 598:359–363. <https://doi.org/10.1038/s41586-021-03911-7>
 56. Sokratian A, Ziaee J, Kelly K, Chang A, Bryant N, Wang S et al (2021) Heterogeneity in α -synuclein fibril activity correlates to disease phenotypes in Lewy body dementia. *Acta Neuropathol* 141:547–564. <https://doi.org/10.1007/s00401-021-02288-1>
 57. Sorrentino ZA, Goodwin MS, Riffe CJ, Dhillon JKS, Xia Y, Gorion KM et al (2019) Unique α -synuclein pathology within the amygdala in Lewy body dementia: implications for disease initiation and progression. *Acta Neuropathol Commun* 7:142. <https://doi.org/10.1186/s40478-019-0787-2>
 58. Spillantini MG, Schmidt ML, Lee VM, Trojanowski JQ, Jakes R, Goedert M (1997) Alpha-synuclein in Lewy bodies. *Nature* 388:839–840. <https://doi.org/10.1038/42166>
 59. Szklarczyk D, Gable AL, Nastou KC, Lyon D, Kirsch R, Pyysalo S et al (2021) The STRING database in 2021: customizable protein–protein networks, and functional characterization of user-uploaded gene/measurement sets. *Nucleic Acids Res* 49:D605–D612. <https://doi.org/10.1093/nar/gkaa1074>
 60. Tang JX, Thompson K, Taylor RW, Oláhová M (2020) Mitochondrial OXPHOS biogenesis: co-regulation of protein synthesis, import, and assembly pathways. *Int J Mol Sci* 21:3820. <https://doi.org/10.3390/ijms21113820>
 61. Telling GC, Parchi P, DeArmond SJ, Cortelli P, Montagna P, Gabizon R et al (1996) Evidence for the conformation of the pathologic isoform of the prion protein enciphering and propagating prion diversity. *Science* (80-) 274:2079–2082. <https://doi.org/10.1126/science.274.5295.2079>
 62. Tyanova S, Temu T, Cox J (2016) The MaxQuant computational platform for mass spectrometry-based shotgun proteomics. *Nat Protoc* 11:2301–2319. <https://doi.org/10.1038/nprot.2016.136>
 63. Tyanova S, Temu T, Sinitcyn P, Carlson A, Hein MY, Geiger T et al (2016) The Perseus computational platform for comprehensive analysis of (prote)omics data. *Nat Methods* 13:731–740. <https://doi.org/10.1038/nmeth.3901>
 64. Vizcaíno JA, Deutsch EW, Wang R, Csordas A, Reisinger F, Ríos D et al (2014) ProteomeXchange provides globally coordinated proteomics data submission and dissemination. *Nat Biotechnol* 32:223–226. <https://doi.org/10.1038/nbt.2839>
 65. Woerman AL (2021) Strain diversity in neurodegenerative disease: an argument for a personalized medicine approach to diagnosis and treatment. *Acta Neuropathol*. <https://doi.org/10.1007/s00401-021-02311-5>
 66. Yang Y, Arseni D, Zhang W, Huang M, Lövestam S, Schweighauser M et al (2022) Cryo-EM structures of amyloid- β 42

- filaments from human brains. *Science* (80-) 375:167–172. <https://doi.org/10.1126/science.abm7285>
67. Zhang H, Duan C, Yang H (2014) Defective Autophagy in Parkinson's Disease: Lessons from Genetics. *Mol Neurobiol* 1:89–104. <https://doi.org/10.1007/s12035-014-8787-5>
68. Zhou Y, Zhou B, Pache L, Chang M, Khodabakhshi AH, Tanaseichuk O et al (2019) Metascape provides a biologist-oriented resource for the analysis of systems-level datasets. *Nat Commun* 10:1523. <https://doi.org/10.1038/s41467-019-09234-6>

Publisher's Note Springer Nature remains neutral with regard to jurisdictional claims in published maps and institutional affiliations.